Molecular Pharmacology Fast Forward. Published on August 9, 2019 as DOI: 10.1124/mol.119.116772
This article has not been copyedited and formatted. The final version may differ from this version.

MOL # 116772

Title: **Calcium-sensing receptor internalization is β-arrestin-dependent and modulated by allosteric ligands**

Authors: Iris Mos[‡,1], Stine E. Jacobsen[‡,1], Simon R. Foster[‡,#], Hans Bräuner-Osborne[‡]

[‡]Department of Drug Design and Pharmacology, Faculty of Health and Medical Sciences, University of Copenhagen, Denmark

[#]Current address: Monash Biomedicine Discovery Institute, Department of Biochemistry & Molecular Biology, Monash University, Australia

Molecular Pharmacology Fast Forward. Published on August 9, 2019 as DOI: 10.1124/mol.119.116772
This article has not been copyedited and formatted. The final version may differ from this version.

MOL # 116772

Running title: **Real-time internalization of the calcium-sensing receptor**

Corresponding author:

Prof. Hans Bräuner-Osborne

Department of Drug Design and Pharmacology

Faculty of Health and Medical Sciences

University of Copenhagen

Universitetsparken 2

DK-2100 Copenhagen, Denmark

Telephone: +45-35334469

Fax: +45-35336041

E-mail: hbo@sund.ku.dk

Text pages:

Tables: 0

Figures: 8

References: 63

Word counts:

Abstract: 242

Introduction: 630

Discussion: 1306

Abbreviations: β_2AR, β_2-adrenergic receptor; CaSR, calcium-sensing receptor; cAMP, 3´5´-cyclic adenosine monophosphate; dFBS, dialyzed fetal bovine serum; DMEM, Dulbecco's modified eagle medium; DMSO, Dimethyl sulfoxide; DPBS, Dulbecco's phosphate buffered saline; ELISA, Enzyme-linked Immunosorbent Assay; $GABA_B$, gamma-aminobutyric acid type B; GIP, glucose-dependent

Molecular Pharmacology Fast Forward. Published on August 9, 2019 as DOI: 10.1124/mol.119.116772
This article has not been copyedited and formatted. The final version may differ from this version.

insulinotropic polypeptide; GLP-1R, glucagon-like peptide 1 receptor; GPCR, G protein-coupled receptor; HBSS, Hank's balanced salt solution; HEK, Human embryonic kidney; IBMX, Isobutyl-1-methyl-xanthine; IP_1, inositol monophosphate; mGlu5, metabotropic glutamate receptor subtype 5; NAM, Negative allosteric modulator; PAM, Positive allosteric modulator; PTH, parathyroid hormone; PTHrP, parathyroid hormone-related protein; PTX, Pertussis toxin; RT, room temperature; TR-FRET, Time-resolved fluorescence resonance energy transfer;

Molecular Pharmacology Fast Forward. Published on August 9, 2019 as DOI: 10.1124/mol.119.116772
This article has not been copyedited and formatted. The final version may differ from this version.

Abstract

G protein-coupled receptor (GPCR) internalization is crucial for the termination of GPCR activity and in some cases associated with G protein-independent signaling and endosomal receptor signaling. To date, internalization has been studied in great detail for class A GPCRs, whereas it is not well established to what extent the observations can be generalized to class C GPCRs including the extracellular calcium-sensing receptor (CaSR).

The CaSR is a prototypical class C GPCR that maintains stable blood calcium (Ca^{2+}) levels by sensing minute changes in extracellular free Ca^{2+}. It is thus necessary that the activity of CaSR is tightly regulated, even whilst continuously being exposed to its endogenous agonist. Previous studies have utilized overexpression of intracellular proteins involved in GPCR trafficking, pathway inhibitors and cell-surface expression or functional desensitization as indirect measures to investigate CaSR internalization. However, there is no general consensus on the processes involved and the mechanism of CaSR internalization remains poorly understood.

The current study provides new insights into the internalization mechanism of CaSR. We have utilized a state-of-the-art TR-FRET-based internalization assay to directly measure CaSR internalization in real-time. We demonstrate that CaSR displays both constitutive and concentration-dependent Ca^{2+}-mediated internalization. For the first time, we conclusively show that CaSR internalization is sensitive to immediate positive and negative modulation by the CaSR-specific allosteric modulators NPS R-568 and NPS 2143, respectively. In addition, we provide compelling evidence that CaSR internalization is β-arrestin-dependent while interestingly being largely independent of $G_{q/11}$ and $G_{i/o}$ protein signaling.

Molecular Pharmacology Fast Forward. Published on August 9, 2019 as DOI: 10.1124/mol.119.116772
This article has not been copyedited and formatted. The final version may differ from this version.

Introduction

The extracellular calcium-sensing receptor (CaSR) is a widely expressed class C G protein-coupled receptor (GPCR) that is essential for calcium homeostasis in the human body through regulation of the synthesis and secretion of the calcium-elevating parathyroid hormone (PTH) (Brown *et al.*, 1993; Brown, 2013). Several natural occurring CaSR mutations have been identified in patients suffering from calcium homeostasis-related disorders (e.g. familial hypocalciuric hypercalcemia and autosomal dominant hypocalcemia), thereby making CaSR an attractive drug target in diseases related to calcium and PTH imbalance (Brown, 2007; Hannan and Thakker, 2013). In 2004, the CaSR-specific positive allosteric modulator (PAM) cinacalcet was the first allosteric GPCR drug to be approved for clinical use. Cinacalcet effectively lowers elevated PTH levels in disorders linked to hyperparathyroidism (Nemeth and Goodman, 2016). Recently, the CaSR PAM etelcalcetide received regulatory approval for clinical use as a more efficacious alternative for cinacalcet with higher level of compliance (Block *et al.*, 2017; Patel and Bridgeman, 2018; Xipell *et al.*, 2019). CaSR expression in tissues unrelated to calcium homeostasis suggest that this receptor could also be a potential therapeutic target for cardiovascular diseases, infertility and cancer (Ellinger, 2016; Tennakoon *et al.*, 2016; Guo *et al.*, 2018). Nevertheless, the precise contribution of CaSR in these disease contexts remains uncertain.

GPCR endocytosis – commonly referred to as GPCR internalization – is a highly regulated process for removal of GPCRs from the cell membrane into intracellular compartments. Given the direct influence on GPCR cell-surface expression, understanding the mechanism(s) of internalization is of crucial importance for obtaining a full comprehension of GPCR signaling and function (Drake *et al.*, 2006; Moore *et al.*, 2007). Internalization has been extensively studied in class A GPCRs, where the most prevalent mechanism after receptor activation includes kinase-mediated phosphorylation of the GPCR C-terminus and intracellular loops followed by β-arrestin recruitment and dynamin-driven internalization in clathrin-coated pits (Moore *et al.*, 2007). However, the internalization mechanism(s) in class B and C GPCRs remain less well-described.

Molecular Pharmacology Fast Forward. Published on August 9, 2019 as DOI: 10.1124/mol.119.116772
This article has not been copyedited and formatted. The final version may differ from this version.

In particular, the processes that underscore internalization of class C GPCRs, including CaSR, are poorly understood and there is a lack of consensus in the current literature. Some studies conclude that CaSR can internalize and recycle to the cell-surface independently of agonist activation (Reyes-Ibarra *et al.*, 2007; Zhuang *et al.*, 2012), whereas others have reported agonist-mediated internalization (Pi *et al.*, 2005; Lorenz *et al.*, 2007). Additionally, Grant *et al.* state that constitutive (i.e. ligand-independent) CaSR internalization is primarily followed by degradation rather than recycling (Grant *et al.*, 2011). Regarding the mechanism underlying CaSR internalization, Pi *et al.* and Lorenz *et al.* have conducted overexpression and inhibition studies of intracellular proteins related to GPCR trafficking, in which cell-surface expression was used as an indirect measure of internalization. Both studies found that CaSR interaction with kinases and β-arrestins was essential for functional desensitization, but not for CaSR internalization (Pi *et al.*, 2005; Lorenz *et al.*, 2007). Furthermore, by using non-specific internalization inhibitors Holstein *et al.* have shown that a PAM may regulate CaSR internalization, although this remains to be shown via direct measurement of CaSR internalization (Holstein *et al.*, 2004).

In the present study, we aimed to delineate the mechanism underlying CaSR internalization and to directly measure the effects of allosteric ligands on CaSR internalization using a real-time time-resolved fluorescence resonance energy transfer (TR-FRET)-based internalization assay (Foster and Bräuner-Osborne, 2018). This assay has previously been applied to directly measure constitutive and agonist-mediated internalization for receptors across different GPCR classes, including the class A ß$_2$-adrenergic receptor (β_2AR) (Roed *et al.*, 2014), class B glucagon-like peptide 1 receptor (GLP-1R) (Roed *et al.*, 2014, 2015) and class C GPRC6A (Jacobsen *et al.*, 2017a). By using CaSR mutants, selective G protein inhibitors and β-arrestin1/2 and $G_{q/11}$ protein knock-out cell lines, we demonstrate that CaSR internalization is β-arrestin-dependent, largely $G_{i/o}$ and $G_{q/11}$ protein-independent and modulated by allosteric ligands.

Molecular Pharmacology Fast Forward. Published on August 9, 2019 as DOI: 10.1124/mol.119.116772
This article has not been copyedited and formatted. The final version may differ from this version.

Materials and Methods

Materials

Unless stated otherwise, all reagents were from Sigma-Aldrich (St. Louis, MO, USA). Dulbecco's Modified Eagle Medium (DMEM), dialyzed Fetal Bovine Serum (dFBS), a mixture of 10,000 units/mL penicillin and 10,000 µg/mL streptomycin, Dulbecco's Phosphate Buffered Saline (DPBS) without Ca^{2+} and Mg^{2+}, Opti-MEM, Hank's Balanced Salt Solution (HBSS) without Ca^{2+}, Mg^{2+} and phenol red, Lipofectamine 2000 and Pertussis toxin (PTX) were from Thermo Fisher Scientific (Waltham, MA, USA). The allosteric modulator NPS R-568 hydrochloride was purchased from Tocris Bioscience (Bristol, UK) and NPS 2143 hydrochloride was synthesized in-house as previously published (Johansson *et al.*, 2013). The selective $G_{q/11}$ inhibitor YM-254890 was purchased from Wako Chemicals GmbH (Neuss, DE). The $G_{q/11}$ knock-out ($G_{q/11}$ KO) and β-arrestin1/2 knock-out (β-arrestin1/2 KO) cells were generated from human embryonic kidney (HEK) 293A cells using CRISPR/Cas9 technology as previously described (Schrage *et al.*, 2015; Alvarez-Curto *et al.*, 2016).

Plasmid DNA constructs

The FLAG-SNAP-tagged β_2AR pEGFPN1 and FLAG-SNAP-tagged GLP-1R pEGFPN1 constructs were a kind gift from Dr. Maria Waldhoer, InterAx Biotech AG (Roed *et al.*, 2014). These constructs contain an upstream sequence encoding a T-cell CD8A signal peptide followed by a FLAG and SNAP tag. The N-terminal FLAG and SNAP tag were inserted to allow expression analysis and real-time internalization measurements, respectively. FLAG-SNAP-tagged CaSR wild-type (WT) and mutant vectors were generated by replacing the GLP-1R sequence of the FLAG-SNAP-tagged GLP-1R pEGFPN1 construct with the CaSR WT, CaSR S170A or CaSR E837A sequence using the MluI-NotI restriction sites. The FLAG-SNAP-tagged CaSR WT and mutant constructs were validated using an inositol monophosphate (IP_1) accumulation assay (Figure 1A) and expression analysis (Figure 1B).

Molecular Pharmacology Fast Forward. Published on August 9, 2019 as DOI: 10.1124/mol.119.116772
This article has not been copyedited and formatted. The final version may differ from this version.

Constructs containing human β-arrestin1 (GenBank accession no. NM_004041.4) and β-arrestin2 (GenBank accession no. NM_004313.3) were made in-house as previously published (Gabe *et al.*, 2018).

Cell culture and transfection

HEK293T, HEK293A, $G_{q/11}$ KO and β-arrestin1/2 KO cells were cultured at 37 ºC and 5% CO_2 in DMEM supplemented with 10% dFBS and 1% penicillin/streptomycin mixture. All cell lines were confirmed as negative for mycoplasma contamination using the LookOut® Mycoplasma PCR detection kit (Sigma-Aldrich, St. Louis, MO, USA). 48 h prior to assays, cells were transiently transfected at a density of 17,000 cells/well in poly-D-lysine coated 96-well plates. White opaque 96-well culture plates (PerkinElmer, Waltham, MA, USA) were used for enzyme-linked immunosorbent assay (ELISA) and clear tissue culture treated 96-well plates (Corning, Corning, NY, USA) for IP_1 and 3´5´-cyclic adenosine monophosphate (cAMP) accumulation assays. For the TR-FRET-based internalization assay, cells were transiently transfected in white 96-well culture plates (Corning, Corning, NY, USA). For each well, 30 ng CaSR construct diluted in 25 µL Opti-MEM was added to 0.25 µL Lipofectamine 2000 diluted in 25 µL Opti-MEM after 5 min incubation at room temperature (RT). For β-arrestin co-expression studies, cells were transfected with a total of 60 ng/well at a CaSR:empty pEGFPN1 vector ratio of 1:1 as negative control and CaSR:β-arrestin ratio of 1:1 and 2:1:1 for co-expression with one or both β-arrestin subtypes, respectively. For the CaSR signaling and expression experiments in HEK293A and β-arrestin1/2 KO cells presented in Figure 8, the HEK293A cells were transfected with a total of 30 ng/well at a CaSR:empty pEGFPN1 vector ratio of 1:3. The DNA:Lipofectamine mixture was subsequently mixed and incubated at RT for 20 min prior to addition to the assay plate (50 µL/well). Next, 100 µL/well of cells diluted in culture media (17,000 cells/well) was added and the assay plate was incubated for 48 h at 37 ºC and 5% CO_2.

Enzyme-linked immunosorbent assay (ELISA) for cell-surface expression

Molecular Pharmacology Fast Forward. Published on August 9, 2019 as DOI: 10.1124/mol.119.116772
This article has not been copyedited and formatted. The final version may differ from this version.

Cell-surface expression levels of the WT and mutant CaSR constructs were examined using ELISA as described previously (Nørskov-Lauritsen *et al.*, 2015). To ensure correct cell-surface labeling, the gamma-aminobutyric acid type B ($GABA_B$) receptor expression system was utilized as a control. In brief, cells were fixed with 4% paraformaldehyde in DPBS for 5 min at RT and washed twice using wash buffer (DPBS supplemented with 1 mM $CaCl_2$ and 1 mM $MgCl_2$). After fixation, all wells were incubated for at least 30 min at RT in blocking solution (ultrapure MilliQ water, 3% skim milk, 1 mM $CaCl_2$, 1 mM $MgCl_2$ 50 mM Trizma hydrochloride solution, pH 7.4) followed by incubation for 45 min with monoclonal anti-FLAG antibody (Sigma-Aldrich, St. Louis, MO, USA) diluted 1:100,000 in blocking solution. Subsequently, cells were incubated for 45 min with horseradish peroxidase-conjugated anti-mouse IgG antibody (Vector Laboratories Inc., Burlingame, CA, USA) diluted 1:2000 in blocking solution after which they were washed four times in blocking solution and four times in wash buffer. Chemiluminescence was measured on an EnSpire plate reader (PerkinElmer, Waltham, MA, USA) immediately after addition of 10 µL/well SuperSignal ELISA Femto Substrate (Thermo Fisher Scientific Waltham, MA, USA).

Inositol monophosphate (IP_1) accumulation assay

IP_1 accumulation downstream of CaSR activation was measured using the HTRF® IP-One assay kit (Cisbio Bioassays, Codolet, France) as previously published (Jacobsen *et al.*, 2017b). In brief, cells were washed once in 100 µL/well of assay buffer (HBSS, 20 mM HEPES, pH 7.4) prior to ligand stimulation for 30 min at 37 ºC. All ligands were prepared in ligand buffer (HBSS, 20 mM HEPES, pH 7.4 supplemented with 20 mM LiCl). Unless stated otherwise, studies with allosteric modulators or the $G_{q/11}$ inhibitor YM-254890, cells were pre-incubated for 30 min at 37 ºC prior to ligand stimulation in ligand buffer supplemented with allosteric modulator or inhibitor and a final dimethyl sulfoxide (DMSO) concentration below 0.1%. After ligand stimulation, the cells were washed with assay buffer (100 µL/well) and subsequently lysed for 30 min at RT using 30 µL/well IP-One Conjugate & Lysis

Molecular Pharmacology Fast Forward. Published on August 9, 2019 as DOI: 10.1124/mol.119.116772
This article has not been copyedited and formatted. The final version may differ from this version.

buffer (Cisbio Bioassays, Codolet, France). The lysed cells were diluted with 30 µL/well assay buffer and 10 µL/well was transferred to a white 384-well Optiplate (PerkinElmer, Waltham, MA, USA). Next, 10 µL/well of detection solution (assay buffer + 2.5% IP_1-d2 conjugate + 2.5% anti-IP_1 antibody Tb^{2+} cryptate) was added and the plate was incubated in the dark for 1 h at RT prior to measurement on an EnVision multimode plate reader (PerkinElmer, Waltham, MA, USA). Emission at 615 and 665 nm were measured upon excitation at 340 nm. The resulting FRET ratios (615/665 nm) were converted to IP_1 concentrations through standard curve interpolation of an IP_1 calibrator provided with the assay kit.

3´5´-Cyclic adenosine monophosphate (cAMP) accumulation assay

CaSR-dependent cAMP inhibition was measured using the cAMP dynamic 2 assay kit purchased from Cisbio Bioassays (Codolet, France). For PTX treatment, cells were pre-treated with 80 ng/mL PTX 24 h prior to assay. Ligands were prepared in ligand buffer (HBSS, 20 mM HEPES, pH 7.4 supplemented with 50 µM IBMX and 0.05% DMSO) containing 1.5 µM forskolin. On the day of the assay, cells were washed once with 100 µL/well assay buffer (HBSS, 20 mM HEPES, pH 7.4) followed by ligand stimulation (50 µL/well) for 30 min at RT. After ligand stimulation, the cells were washed once with 100 µL/well assay buffer and were then lysed for 30 min at RT using 30 µL/well cAMP Lysis & Detection Buffer. The lysates were diluted with 30 µL/well assay buffer and 10 µL/well was transferred to a white small-volume 384-well plate (Greiner Bio-One, Monroe, USA). 10 µL/well detection solution (assay buffer + 2.5% cAMP-d2 conjugate + 2.5% anti-cAMP antibody Eu^{3+} cryptate) was added and the plate was incubated in the dark for 1 h at RT prior to measurement on an EnVision multimode plate reader (PerkinElmer, Waltham, MA, USA). Emission at 615 and 665 nm were measured upon excitation at 340 nm. The resulting FRET ratios (615/665 nm) were converted to cAMP concentrations through standard curve interpolation of a cAMP calibrator provided with the assay kit.

TR-FRET-based real-time internalization assay

Molecular Pharmacology Fast Forward. Published on August 9, 2019 as DOI: 10.1124/mol.119.116772
This article has not been copyedited and formatted. The final version may differ from this version.

CaSR internalization was measured using a TR-FRET (Time-Resolved Fluorescence Resonance Energy Transfer) based real-time internalization assay as previously published (Roed *et al.*, 2014, 2015; Levoye *et al.*, 2015; Jacobsen *et al.*, 2017a; Foster and Bräuner-Osborne, 2018; Gabe *et al.*, 2018). For each well, cell-surface expressed SNAP-tagged receptors were labeled for 1 h with 50 µL 0.1 nM cell-impermeable donor fluorophore (SNAP lumi4®-Tb, Cisbio Bioassays, Codolet, France) diluted in Opti-MEM. Labeling was performed at 4 ºC to allow visualization of constitutive internalization, as done previously for the class C GPCR GPRC6A (Jacobsen *et al.*, 2017a). All ligands were prepared at 2x final concentration in assay buffer (HBSS, 20 mM HEPES, pH 7.4), while the acceptor fluorophore (fluorescein-O-acetic acid) was diluted in assay buffer to a final concentration of 40 nM. The prepared ligand and acceptor fluorophore solutions were pre-heated to 37 ºC prior to addition. After labeling, cells were washed twice with 100 µL/well cold assay buffer. Subsequently, 50 µL/well ligand and 50 µL/well 40 nM fluorescein-O-acetic acid solution were added and internalization was measured immediately at 37 ºC on an EnVision multimode plate reader (PerkinElmer, Waltham, MA, USA). Emission at 615 and 520 nm were measured every 6 min upon excitation at 340 nm. The level of internalization depicted in the figures represents the donor over acceptor emission ratio (615/520 nm). When testing EDTA or YM-254890, the reagents were present in final concentration during both labeling and real-time measurements. When testing PTX, cells were pre-treated for 24 h with 80 ng/mL PTX prior to assay.

Data analysis

Curve fitting and statistical analyses were performed with Graphpad Prism 7 (Graphpad Software, San Diego, CA). Concentration-response curves were fitted using the following four-parameter nonlinear regression equation:

$$Response = \frac{Bottom + (top - bottom)}{(1 + 10^{(logEC_{50} - \log[agonist])^n})}$$

Molecular Pharmacology Fast Forward. Published on August 9, 2019 as DOI: 10.1124/mol.119.116772
This article has not been copyedited and formatted. The final version may differ from this version.

In this equation, top and bottom are the response values obtained at the top and bottom plateau of the concentration-response curve. The EC_{50} value is defined as the agonist concentration necessary to elicit a half-maximal response and the n value corresponds to the hill slope. For internalization data, each real-time trace was baseline-corrected prior to area under the curve (AUC) measurement. The obtained AUC values were normalized as described in the figure legends. Statistical analyses of were performed using a one-way ANOVA followed by a Dunnett's post-test or Tukey's multiple comparisons test for comparisons against one condition or multiple conditions, respectively. Statistical significance is notated in the figures as: * $P < 0.05$, ** $P < 0.01$, *** $P < 0.001$. For some data points, error bars are not visible as they are smaller than the symbol size.

Molecular Pharmacology Fast Forward. Published on August 9, 2019 as DOI: 10.1124/mol.119.116772
This article has not been copyedited and formatted. The final version may differ from this version.

Results

The N-terminal SNAP-tag does not interfere with CaSR functionality

In this study, CaSR internalization was investigated using CaSR WT and the CaSR mutants S170A and E837A that are located in the L-amino acid and allosteric ligand binding site, respectively. CaSR internalization was assessed using a TR-FRET-based real-time internalization assay that requires the addition of an N-terminal SNAP tag to the receptor of interest. Prior to internalization, the FLAG-SNAP-tagged constructs were validated for their agonist response using an IP_1 accumulation assay (Figure 1A) and for their cell-surface expression using an ELISA (Figure 1B). To investigate whether the SNAP tag interfered with the signaling capacity of CaSR, FLAG-SNAP-tagged CaSR WT was compared with HA-tagged CaSR WT, which we have previously characterized in detail (Jacobsen *et al.*, 2017b). In a functional IP_1 accumulation assay there was no difference in agonist potency of Ca^{2+} for the two receptor constructs (Figure 1A; pEC_{50} values of 2.50 ± 0.02 and 2.39 ± 0.03 for FLAG-SNAP-CaSR WT and HA-CaSR WT, respectively), thereby confirming that the SNAP tag did not prevent Ca^{2+}-mediated activation of the $G_{q/11}$ pathway. We next used the FLAG-SNAP-CaSR construct to study Ca^{2+}-mediated CaSR internalization.

CaSR displays constitutive and Ca^{2+}-mediated internalization

CaSR internalization was measured in the absence and presence of its endogenous agonist Ca^{2+} and internalization was observed under both conditions (Figure 2A). Increasing Ca^{2+} concentrations induced internalization in a concentration-dependent manner (pEC_{50} of 2.48 ± 0.04) (Figure 2B). Direct comparison to the IP_1 accumulation data (Figure 1A) revealed that Ca^{2+} triggers internalization and $G_{q/11}$-mediated activity of CaSR with equal potency.

The physiological ligands of CaSR include essential components of cell culture media and assay buffers such as divalent cations (e.g. Ca^{2+}, Mg^{2+}) and L-amino acids (e.g. L-phenylalanine, L-

Molecular Pharmacology Fast Forward. Published on August 9, 2019 as DOI: 10.1124/mol.119.116772
This article has not been copyedited and formatted. The final version may differ from this version.

tryptophan). Additionally, cells are able to release such ligands either through passive or active membrane transport (Thomsen *et al.*, 1994; Hoenderop and Bindels, 2005). To determine whether the constitutive internalization was mediated by divalent cations and/or L-amino acids released from the cells during the real-time assay, we employed two strategies. First, EDTA was used to chelate extracellular cations present during the internalization assay. Since L-amino acids require the presence of Ca^{2+} for activating CaSR, chelation of Ca^{2+} by EDTA also indirectly eliminates the amino acid-induced effects (Conigrave *et al.*, 2000; Geng *et al.*, 2016). To test if EDTA had non-specific activity on the cells or assay, we used FLAG-SNAP-β_2AR as a control. As shown in Figure 2C and 2D, 1 mM EDTA significantly reduced the level of isoproterenol-mediated internalization ($p < 0.01$, one-way ANOVA followed by a Tukey's multiple comparisons test) while 0.5 mM EDTA had no effect. Hence, 0.5 mM EDTA was used during labeling and real-time internalization measurements of CaSR. The usage of 0.5 mM EDTA did not affect constitutive internalization of CaSR (Figure 2E and 2F). These results indicate that constitutive internalization is not caused by ambient divalent cations and L-amino acids but rather is an inherent property of CaSR.

Secondly, constitutive internalization was investigated using a CaSR loss-of-function mutant, S170A. The S170 residue is located in the highly conserved L-amino acid orthosteric binding site, where it directly interacts with L-Trp according to the crystal structures of the CaSR extracellular domain (Geng *et al.*, 2016; Zhang *et al.*, 2016). Mutating this residue has been shown to prevent Ca^{2+}-mediated signaling of CaSR (Bräuner-Osborne *et al.*, 1999; Geng *et al.*, 2016). In agreement with the literature, FLAG-SNAP-CaSR S170A abolished Ca^{2+}-mediated IP_1 accumulation (Figure 1A). Cell-surface expression analysis by ELISA verified that the loss of Ca^{2+}-mediated activity was not caused by a lack of cell-surface expression. The surface expression of CaSR S170A was marginally reduced relative to CaSR WT, however this alone could not explain the loss of function (Figure 1B, $p < 0.001$, one-way ANOVA followed by a Dunnett's post-test). In the internalization assay, CaSR S170A internalized constitutively while no Ca^{2+}-mediated internalization was observed (Figure 2G and 2H). Moreover, constitutive internalization of CaSR S170A was unaffected by the presence of 0.5 mM

Molecular Pharmacology Fast Forward. Published on August 9, 2019 as DOI: 10.1124/mol.119.116772
This article has not been copyedited and formatted. The final version may differ from this version.

EDTA. Thus, the constitutive internalization was not eliminated by mutating the orthosteric ligand binding site or by chelation of extracellular ambient Ca^{2+}. These results strongly suggest that CaSR displays constitutive internalization.

Ca^{2+}-mediated CaSR internalization is modulated by allosteric ligands

To study the effect of allosteric ligands on CaSR internalization, we measured internalization in the presence of the representative NAM NPS 2143 or PAM NPS R-568 (Figure 3). Ca^{2+}-mediated internalization of CaSR was reduced in the presence of 5 μM NPS 2143 and enhanced in the presence of 5 μM NPS R-568. This concentration of NPS 2143 and NPS R-568 was found to fully inhibit or potentiate the Ca^{2+}-induced CaSR response in the IP_1 accumulation assay, respectively (Figure 4A and 5A).

CaSR-specific NAMs and PAMs generally share an overlapping binding site in the seven-transmembrane domain. Previous publications have revealed that the modulating effects from both NPS 2143 and NPS R-568 can be eliminated by mutating the E837 residue situated within this overlapping binding site (Hu *et al.*, 2002, 2006; Petrel *et al.*, 2004; Jacobsen *et al.*, 2017b). To determine if the observed modulation of CaSR internalization was directly mediated by the NAM and PAM, internalization and functional testing were performed with FLAG-SNAP-CaSR E837A.

CaSR E837A cell-surface expression was equivalent to CaSR WT as demonstrated by ELISA (Figure 1B). Moreover, the Ca^{2+}-induced effect on CaSR E837A was similar to CaSR WT in both the IP_1 accumulation assay (Figure 1A) and the real-time internalization assay (Figure 3D and 3E). Thus, mutating E837 did not affect surface expression or Ca^{2+}-mediated receptor activation and internalization.

Molecular Pharmacology Fast Forward. Published on August 9, 2019 as DOI: 10.1124/mol.119.116772
This article has not been copyedited and formatted. The final version may differ from this version.

In accordance with previously published studies, the E837A mutant did prevent NPS 2143-mediated inhibition and NPS R-568-mediated potentiation of Ca^{2+}-induced IP_1 accumulation (Figure 4B and 5B). When tested in the real-time internalization assay, the modulating effects of NPS 2143 and NPS R-568 were likewise abolished for the Ca^{2+}-mediated internalization of CaSR E837A (Figure 4E, 4F, 5E and 5F), while the Ca^{2+}-mediated internalization of CaSR WT was subjected to NPS 2143-induced inhibition and NPS R-568-induced potentiation as expected (Figure 4C, 4D, 5C and 5D). Furthermore, a small yet statistically significant increase in constitutive internalization from NPS R-568 (Figure 5D, $p < 0.05$, one-way ANOVA followed by a Tukey's multiple comparisons test) was abrogated in CaSR E837A (Figure 5D and 5F). These data demonstrate that the CaSR-specific NAM NPS 2143 and PAM NPS R-568 are directly responsible for the modulation of CaSR internalization.

Constitutive and Ca^{2+}-mediated CaSR internalization is independent of G protein activation

It is widely accepted that CaSR interacts with the $G_{q/11}$ and $G_{i/o}$ protein families, although interaction with other G proteins has also been reported (Thomsen *et al.*, 2012). To elucidate the mechanism of CaSR internalization, we investigated whether activation of these G proteins drive CaSR internalization. Commercially available natural products YM-254890 and pertussis toxin (PTX) were used to inhibit $G_{q/11}$- and $G_{i/o}$-mediated activity, respectively (Campbell and Smrcka, 2018). As seen in Figure 6A, 30 min pre-incubation with 1 μM YM-254890 to block $G_{q/11}$-dependent signaling reduced Ca^{2+}-mediated IP_1 generation via CaSR WT to the basal IP_1 level. Similarly, the Ca^{2+}-mediated decrease in cAMP accumulation was abrogated by 24 h pre-incubation with 80 ng/mL PTX (Figure 6B).

Both G protein inhibitors did not affect constitutive CaSR internalization (Figure 6C and 6D, open symbols). Pre-incubation with PTX had no effect on Ca^{2+}-mediated internalization while a modest 20% decrease was observed in the presence of YM-254890 (Figure 6C and 6D, closed symbols, $p < 0.05$, one-way ANOVA followed by a Dunnett's post-test). Pre-incubation with PTX and YM-254890

Molecular Pharmacology Fast Forward. Published on August 9, 2019 as DOI: 10.1124/mol.119.116772
This article has not been copyedited and formatted. The final version may differ from this version.

did not further suppress Ca^{2+}-mediated internalization demonstrating that the two G protein families do not compensate for each other.

As presented in Figures 6E-G, similar results were obtained in CRISPR/Cas9 edited HEK293A cells lacking the $G_{q/11}$ protein ($G_{q/11}$ KO cells). In particular, both the constitutive and Ca^{2+}-mediated internalization were maintained in the $G_{q/11}$ KO cells, consistent with the pharmacologically blocked $G_{q/11}$ in YM-254890-treated HEK293A cells. Overnight PTX treatment in the $G_{q/11}$ KO cells led to a slight reduction in Ca^{2+}-mediated internalization, but did not affect the constitutive internalization (Figure 6E-G). Collectively, these results suggest that constitutive and Ca^{2+}-mediated CaSR internalization is largely independent of $G_{q/11}$ or $G_{i/o}$ activation.

CaSR internalization is predominantly driven by β-arrestin

To investigate the involvement of β-arrestin, CaSR internalization was measured in a CRISPR/Cas9 edited cell line lacking β-arrestin1 and β-arrestin2 (β-arrestin1/2 KO) (O'Hayre *et al.*, 2017). By expressing CaSR in both the β-arrestin1/2 KO cell line and its parental cell line HEK293A, it was demonstrated that constitutive internalization of CaSR was reduced, while the Ca^{2+}-mediated internalization of CaSR was abolished in the absence of β-arrestins (Figure 7A) despite having equivalent surface labeling of CaSR in both cell lines (data not shown).

To validate that the loss of Ca^{2+}-mediated internalization was caused by the lack of β-arrestin expression, the two β-arrestin subtypes were transiently expressed in the β-arrestin1/2 KO cell line and CaSR internalization was measured. The introduction of each β-arrestin subtype did not affect CaSR surface labeling (data not shown). Constitutive internalization was significantly enhanced by both β-arrestin1 and β-arrestin2 (Figure 7B and 7D, one-way ANOVA followed by a Dunnett's post-test). Furthermore, the re-introduction of either β-arrestin1, β-arrestin2 or both β-arrestins restored Ca^{2+}-

mediated internalization in the β-arrestin1/2 KO cells (Figure 7C and 7D). These results demonstrate that CaSR internalization is largely β-arrestin-dependent.

In this study, NPS 2143 and NPS R-568 have been shown to affect not only CaSR signaling but also internalization. The question remains whether these allosteric ligands modulate Ca^{2+}-mediated CaSR signaling because they modulate internalization or vice versa. To investigate this, we measured the immediate effects of NPS 2143 and NPS R-568 on CaSR signaling in β-arrestin1/2 KO cells, where Ca^{2+}-mediated internalization was shown to be abolished (Figure 8A). Despite a slightly higher cell-surface expression (Figure 8B), the maximum Ca^{2+}-induced IP_1 accumulation response in the β-arrestin1/2 KO cells was lower than observed with the HEK293A cells. However, NPS 2143 and NPS R-568 were still able to qualitatively modulate CaSR signaling in the β-arrestin1/2 KO cell line to the same extent as in the parental HEK293A cell line. Thus, removal of β-arrestin1/2 and thereby Ca^{2+}-mediated internalization does not impair modulation of CaSR signaling by allosteric ligands.

Molecular Pharmacology Fast Forward. Published on August 9, 2019 as DOI: 10.1124/mol.119.116772
This article has not been copyedited and formatted. The final version may differ from this version.

Discussion

In the present study, we demonstrate that CaSR displays constitutive and Ca^{2+}-mediated internalization that is β-arrestin-dependent and sensitive to allosteric modulators. In accordance with our results, several studies have previously reported that CaSR is constitutively internalized (Reyes-Ibarra *et al.*, 2007; Grant *et al.*, 2011; Zhuang *et al.*, 2012). However, the potential impact of ambient CaSR ligands such as extracellular cations or L-amino acids was not addressed in these studies. In the current study, we have shown that constitutive internalization of CaSR occurs independently of extracellular cations and L-amino acids, as constitutive internalization was not abolished by the chelating agent EDTA or the CaSR loss-of-function mutant S170A.

In order to gain these new insights into CaSR internalization, we have utilized a TR-FRET-based assay, which allows high-throughput, sensitive and readily-quantified detection of receptor internalization in real-time (Foster and Bräuner-Osborne, 2018). This assay provides a useful platform to study the role of β-arrestin and allosteric modulation of CaSR internalization in greater detail than previously. Indeed, there are inconsistencies in the literature about the key processes and proteins involved in CaSR internalization. Reyes-Ibarra *et al.* and Zhuang *et al.* show constitutive CaSR internalization followed by recycling (Reyes-Ibarra *et al.*, 2007; Zhuang *et al.*, 2012), while Grant *et al.* report merely lysosomal degradation (Grant *et al.*, 2011). In other studies, CaSR has been reported to undergo Ca^{2+}-mediated internalization (Pi *et al.*, 2005; Lorenz *et al.*, 2007). These data have been generated using a variety of approaches including receptor truncation/mutations, trafficking and signaling inhibitors (e.g. tunicamycin, gallein) and overexpression or siRNA knockdown of proteins (such as β-arrestin1/2 or GRKs) (Pi *et al.*, 2005; Lorenz *et al.*, 2007; Reyes-Ibarra *et al.*, 2007; Grant *et al.*, 2011, 2015; Zhuang *et al.*, 2012), which likely explain the differences in conclusions drawn. Importantly, the majority of studies have used static measures of CaSR localization, including immunoprecipitation (Reyes-Ibarra *et al.*, 2007) or immunofluorescence-based approaches (Zhuang *et al.*, 2012), or have indirectly tracked CaSR internalization by measuring changes in functional desensitization and/or cell-surface expression (Pi *et al.*, 2005; Lorenz *et al.*, 2007; Grant *et al.*, 2011,

Molecular Pharmacology Fast Forward. Published on August 9, 2019 as DOI: 10.1124/mol.119.116772
This article has not been copyedited and formatted. The final version may differ from this version.

2015). These approaches typically only allow a qualitative measure and not, as in the current study, a detailed quantitative measure of receptor internalization.

NPS R-568 and NPS 2143 are CaSR allosteric modulators with well-characterized pharmacological profiles (Nemeth *et al.*, 1996; Nemeth, 2002), but their effect on CaSR internalization has not been systematically investigated. In the present study, we show that CaSR internalization is negatively and positively modulated by NPS 2143 and NPS R-568, respectively. These results are in agreement with previous findings on other receptors reporting allosteric modulation of ligand-mediated internalization for the class A M1 and M4 muscarinic acetylcholine receptors (Leach *et al.*, 2010; Yeatman *et al.*, 2014), D2 dopamine receptor (Basu *et al.*, 2013), cannabinoid receptor type 1 (Ahn *et al.*, 2012; Laprairie *et al.*, 2015) and the class C metabotropic glutamate receptor 7 (Pelkey *et al.*, 2007). Furthermore, NPS R-568 triggered a small but statistically significant increase in constitutive CaSR internalization. We propose that this could either be caused by positive modulation of the small amounts of ambient agonist present during the assay or by a direct activation of the CaSR internalization pathway.

Additionally, CaSR modulators have been reported to affect the biosynthesis and forward trafficking of WT and mutant CaSR. For NPS 2143 and NPS R-568, a respective decrease or increase in CaSR WT surface expression was obtained following overnight exposure with the allosteric modulators (Huang and Breitwieser, 2007; White *et al.*, 2009; Cavanaugh *et al.*, 2010; Leach *et al.*, 2013). Here we further demonstrate that these modulators affect CaSR internalization in a similar manner, although immediately after agonist stimulation.

CaSR interaction with β-arrestin1 and 2 has previously been shown to be crucial for functional desensitization, but not for Ca^{2+}-mediated internalization (Pi *et al.*, 2005; Lorenz *et al.*, 2007). Pi *et al.* and Lorenz *et al.* utilized a flow cytometry method in which internalization was indirectly measured as a loss in cell-surface expression. In their studies, the potential involvement of β-arrestin was determined

Molecular Pharmacology Fast Forward. Published on August 9, 2019 as DOI: 10.1124/mol.119.116772
This article has not been copyedited and formatted. The final version may differ from this version.

by β-arrestin overexpression, which could mask their importance as endogenously-expressed β-arrestin in the cells could already saturate the internalization pathway. In the present study, we clearly demonstrate the requirement for β-arrestin in Ca^{2+}-mediated CaSR internalization in cells lacking both β-arrestin subtypes. In reciprocal experiments, transfection with either β-arrestin1 or β-arrestin2 recovered internalization of CaSR. Interestingly, both constitutive and Ca^{2+} mediated internalization is largely independent of the $G_{q/11}$ and $G_{i/o}$ signaling pathways indicating that the β-arrestins are recruited independently of the major CaSR G protein pathways.

The CaSR PAM cinacalcet was the first allosteric GPCR modulator to be approved for clinical use. As a result, drug discovery for CaSR-related diseases has shifted interest towards the development of allosteric drugs. To date, a great number of allosteric ligands acting on CaSR have been reported with well-known pharmacological and efficacy and safety profiles in clinical trials, but there is still limited knowledge on the clinical importance of CaSR internalization. For some GPCRs, constitutive internalization and recycling ensures a constant pool of functional receptors at the cellular surface (Hein *et al.*, 1994; Mcdaniel *et al.*, 2012; Basagiannis and Christoforidis, 2016). CaSR is characterized by its constant or prolonged exposure to agonist and thus a persistent cell surface expression of functional receptors is required to retain responsiveness. Accordingly, constitutive internalization and recycling has been observed for CaSR (Reyes-Ibarra *et al.*, 2007; Zhuang *et al.*, 2012) as well as for the related class C mGlu5 receptor (Trivedi and Bhattacharyya, 2012), $GABA_B$ receptor (Grampp *et al.*, 2007; Vargas *et al.*, 2008) and GPRC6A (Jacobsen *et al.*, 2017a). Grant *et al.* propose an alternative strategy for CaSR to remain responsive, in which prolonged Ca^{2+} exposure triggers constitutive internalization followed by degradation rather than recycling. Instead, CaSR from a persistent intracellularly available pool is directed to the cell-surface (Grant *et al.*, 2011). Although we cannot investigate the anterograde trafficking of CaSR as our TR-FRET assay requires labeling of cell-surface expressed receptors, our principal findings on CaSR modulators agree with this hypothesis.

Molecular Pharmacology Fast Forward. Published on August 9, 2019 as DOI: 10.1124/mol.119.116772
This article has not been copyedited and formatted. The final version may differ from this version.

Interestingly, we find that agonist induced IP_1 signaling is reduced in the β-arrestin1/2 KO cell line compared to the parental HEK293A cell line, despite slightly increased receptor cell-surface expression in the former. This is in accordance with recent studies investigating disease-causing mutations of the adaptor protein-2σ subunit (AP2σ) which impair CaSR internalization, increase CaSR cell-surface expression and reduce CaSR signaling (Gorvin *et al.*, 2018). These results suggest that receptor internalization is required to obtain a full IP_1 response, which could be driven by sustained signaling from internalized receptors (Gorvin *et al.*, 2018), or alternatively point to the requirement for receptor internalization, dephosphorylation and recycling to resensitize the receptor for sustained effects (Ward and Riccardi, 2012). However, more studies are needed to delineate the mechanism of this observation. Moreover, we find that the NAM and PAM qualitatively modulate the IP_1 response to the same level in both cell lines demonstrating that PAM/NAM effects on signaling are not downstream of modulating receptor internalization or vice versa.

In conclusion, we demonstrate that CaSR undergoes both constitutive and Ca^{2+}-mediated internalization using a TR-FRET-based real-time internalization assay. Ca^{2+}-mediated CaSR internalization was shown to be concentration-dependent with a Ca^{2+} potency equal to that determined for $G_{q/11}$-mediated IP_1 accumulation. In addition, this study reveals that Ca^{2+}-mediated CaSR internalization is sensitive to allosteric modulation, G protein-independent and largely β-arrestin1/2-dependent. More studies are needed to determine whether β-arrestin and/or G protein involvement is a universal phenomenon or specific to the HEK293 cellular background (i.e. the dependence on expression levels of receptor and intracellular signaling and scaffolding proteins). Future experiments investigating CaSR internalization upon stimulation with other CaSR-specific PAMs and NAMs could determine whether differences in pharmacological profiles can be related to biased signaling and distinct effects on internalization. Overall, these findings contribute to the full delineation of the mechanisms regulating CaSR signaling.

Molecular Pharmacology Fast Forward. Published on August 9, 2019 as DOI: 10.1124/mol.119.116772
This article has not been copyedited and formatted. The final version may differ from this version.

Acknowledgements

We thank Mie F. Pedersen for providing the β-arrestin cDNA constructs and for fruitful discussions regarding the use of β-arrestin1/2 knock-out cells to study GPCR internalization. We thank Dr. Asuka Inoue (Laboratory of Molecular and Cellular Biochemistry and Japan Science and Technology agency, Japan) for the generous gift of the $G_{q/11}$ and ß-arrestin1/2 knock-out cell lines.

Participated in research design: Mos, Jacobsen, Foster, Bräuner-Osborne

Conducted experiments: Mos, Jacobsen

Performed data analysis: Mos, Jacobsen

Wrote or contributed to the writing of the manuscript: Mos, Jacobsen, Foster, Bräuner-Osborne

References

Ahn KH, Mahmoud MM, and Kendall DA (2012) Allosteric modulator ORG27569 induces CB1 cannabinoid receptor high affinity agonist binding state, receptor internalization, and Gi protein-independent ERK1/2 kinase activation. *J Biol Chem* **287**:12070–12082.

Alvarez-Curto E, Inoue A, Jenkins L, Raihan SZ, Prihandoko R, Tobin AB, and Milligan G (2016) Targeted elimination of G proteins and arrestins defines their specific contributions to both intensity and duration of G protein-coupled receptor signaling. *J Biol Chem* **291**:27147–27159.

Basagiannis D, and Christoforidis S (2016) Constitutive endocytosis of VEGFR2 protects the receptor against shedding. *J Biol Chem* **291**:16892–16903.

Basu D, Tian Y, Bhandari J, Jiang JR, Hui P, Johnson RL, and Mishra RK (2013) Effects of the dopamine D2 allosteric modulator, PAOPA, on the expression of GRK2, arrestin-3, ERK1/2, and on receptor internalization. *PLoS One* **8**:1–11.

Block GA, Bushinsky DA, Cheng S, Cunningham J, Dehmel B, Drueke TB, Ketteler M, Kewalramani R, Martin KJ, Moe SM, Patel UD, Silver J, Sun Y, Wang H, and Chertow GM (2017) Effect of etelcalcetide vs cinacalcet on serum parathyroid hormone in patients receiving hemodialysis with secondary hyperparathyroidism: A randomized clinical trial. *JAMA* **317**:156–164.

Bräuner-Osborne H, Jensen AA, Sheppard PO, O'Hara P, and Krogsgaard-Larsen P (1999) The agonist-binding domain of the CaSR is located at the amino-terminal domain. *J Biol Chem* **274**:18382–18386.

Brown EM (2007) Clinical lessons from the calcium-sensing receptor. *Nat Clin Pr Endocrinol Metab* **3**:122–133.

Brown EM (2013) Role of the calcium-sensing receptor in extracellular calcium homeostasis. *Best Pract Res Clin Endocrinol Metab* **27**:333–343.

Brown EM, Gamba G, Riccardi D, Lombardi M, Butters R, Kifor O, Sun A, Hediger MA, Lytton J, and Hebert SC (1993) Cloning and characterization of an extracellular Ca2+-sensing receptor

from bovine parathyroid. *Nature* **366**:575–580.

Campbell AP, and Smrcka A V (2018) Targeting G protein-coupled receptor signalling by blocking G proteins. *Nat Rev Drug Discov* **17**:789–803.

Cavanaugh A, McKenna J, Stepanchick A, and Breitwieser GE (2010) Calcium-sensing receptor biosynthesis includes a cotranslational conformational checkpoint and endoplasmic reticulum retention. *J Biol Chem* **285**:19854–19864.

Conigrave AD, Quinn SJ, and Brown EM (2000) L-amino acid sensing by the extracellular Ca2+-sensing receptor. *Proc Natl Acad Sci U S A* **97**:4814–4819.

Drake MT, Shenoy SK, and Lefkowitz RJ (2006) Trafficking of G protein-coupled receptors. *Circ Res* **99**:570–582.

Ellinger I (2016) The calcium-sensing receptor and the reproductive system. *Front Physiol* **7**.

Foster S, and Bräuner-Osborne H (2018) Investigating internalization and intracellular trafficking of GPCRs: new techniques and real-time experimental approaches. *Handb Exp Pharmacol* **245**:41–61.

Gabe MBN, Sparre-Ulrich AH, Pedersen MF, Gasbjerg LS, Inoue A, Bräuner-Osborne H, Hartmann B, and Rosenkilde MM (2018) Human GIP(3-30)NH2 inhibits G protein-dependent as well as G protein-independent signaling and is selective for the GIP receptor with high-affinity binding to primate but not rodent GIP receptors. *Biochem Pharmacol* **150**:97–107.

Geng Y, Mosyak L, Kurinov I, Zuo H, Sturchler E, Cheng TC, Subramanyam P, Brown AP, Brennan SC, Mun HC, Bush M, Chen Y, Nguyen TX, Cao B, Chang DD, Quick M, Conigrave AD, Colecraft HM, McDonald P, and Fan QR (2016) Structural mechanism of ligand activation in human calcium-sensing receptor. *Elife* **5**:e13662.

Gorvin CM, Rogers A, Hastoy B, Tarasov AI, Frost M, Sposini S, Inoue A, Whyte MP, Rorsman P, Hanyaloglu AC, Breitwieser GE, and Thakker R V (2018) AP2σ mutations impair calcium-sensing receptor trafficking and signaling, and show an endosomal pathway to spatially direct G-protein selectivity. *Cell Rep* **22**:1054–1066.

Grampp T, Sauter K, Markovic B, and Benke D (2007) Gamma-aminobutyric acid type B receptors

are constitutively internalized via the clathrin-dependent pathway and targeted to lysosomes for degradation. *J Biol Chem* **282**:24157–24165.

Grant MP, Cavanaugh A, and Breitwieser GE (2015) 14-3-3 proteins buffer intracellular calcium sensing receptors to constrain signaling. *PLoS One* **10**:1–20.

Grant MP, Stepanchick A, Cavanaugh A, and Breitwieser GE (2011) Agonist-driven maturation and plasma membrane insertion of calcium-sensing receptors dynamically control signal amplitude. *Sci Signal* **4**:ra78.

Guo Y, Yang X, He J, Liu J, Yang S, and Dong H (2018) Important roles of the Ca2+-sensing receptor in vascular health and disease. *Life Sci* **209**:217–227, Elsevier.

Hannan FM, and Thakker R V (2013) Calcium-sensing receptor (CaSR) mutations and disorders of calcium, electrolyte and water metabolism. *Best Pract Res Clin Endocrinol Metab* **27**:359–371, Elsevier Ltd.

Hein L, Ishii K, Coughlin SR, and Kobilka BK (1994) Intracellular targeting and trafficking of thrombin receptors. A novel mechanism for resensitization of a G protein-coupled receptor. *J Biol Chem* **269**:27719–27726.

Hoenderop JG, and Bindels RJ (2005) Epithelial Ca2+ and Mg2+ channels in health and disease. *J Am Soc Nephrol* **16**:15–26.

Holstein DM, Berg KA, Leeb-Lundberg LMF, Olson MS, and Saunders C (2004) Calcium-sensing receptor-mediated ERK1/2 activation requires Gαi2 coupling and dynamin-independent receptor internalization. *J Biol Chem* **279**:10060–10069.

Hu J, Jiang J, Costanzi S, Thomas C, Yang W, Feyen JHM, Jacobson KA, and Spiegel AM (2006) A missense mutation in the seven-transmembrane domain of the human Ca2+ receptor converts a negative allosteric modulator into a positive allosteric modulator. *J Biol Chem* **281**:21558–21565.

Hu J, Reyes-Cruz G, Chen W, Jacobson KA, and Spiegel AM (2002) Identification of acidic residues in the extracellular loops of the seven-transmembrane domain of the human Ca2+ receptor critical for response to Ca2+ and a positive allosteric modulator. *J Biol Chem* **277**:46622–46631.

Huang Y, and Breitwieser GE (2007) Rescue of calcium-sensing receptor mutants by allosteric modulators reveals a conformational checkpoint in receptor biogenesis. *J Biol Chem* **282**:9517–9525.

Jacobsen SE, Ammendrup-Johnsen I, Jansen AM, Gether U, Madsen KL, and Bräuner-Osborne H (2017) The GPRC6A receptor displays constitutive internalization and sorting to the slow recycling pathway. *J Biol Chem* **292**:6910–6926.

Jacobsen SE, Gether U, and Braüner-Osborne H (2017) Investigating the molecular mechanism of positive and negative allosteric modulators in the calcium-sensing receptor dimer. *Sci Rep* **7**:1–14.

Johansson H, Cailly T, Thomsen ARB, Bräuner-Osborne H, and Pedersen DS (2013) Synthesis of the calcilytic ligand NPS 2143. *Beilstein J Org Chem* **9**:1383–1387.

Laprairie RB, Bagher AM, Kelly ME, and Denovan-Wright EM (2015) Cannabidiol is a negative allosteric modulator of the cannabinoid CB1 receptor. *Br J Pharmacol* **172**:4790–4805.

Leach K, Loiacono RE, Felder CC, McKinzie DL, Mogg A, Shaw DB, Sexton PM, and Christopoulos A (2010) Molecular mechanisms of action and in vivo validation of an M4 muscarinic acetylcholine receptor allosteric modulator with potential antipsychotic properties. *Neuropsychopharmacology* **35**:855–869.

Leach K, Wen A, Cook AE, Sexton PM, Conigrave AD, and Christopoulos A (2013) Impact of clinically relevant mutations on the pharmacoregulation and signaling bias of the calcium-sensing receptor by positive and negative allosteric modulators. *Endocrinology* **154**:1105–1116.

Levoye A, Zwier JM, Jaracz-Ros A, Klipfel L, Cottet M, Maurel D, Bdioui S, Balabanian K, Prézeau L, Trinquet E, Durroux T, and Bachelerie F (2015) A broad G protein-coupled receptor internalization assay that combines SNAP-tag labeling, diffusion-enhanced resonance energy transfer, and a highly emissive terbium cryptate. *Front Endocrinol (Lausanne)* **6**:1–11.

Lorenz S, Frenzel R, Paschke R, Breitwieser GE, and Miedlich SU (2007) Functional desensitization of the extracellular calcium-sensing receptor is regulated via distinct mechanisms: Role of G protein-coupled receptor kinases, protein kinase C and β-arrestins. *Endocrinology* **148**:2398–

2404.

Mcdaniel FK, Molden BM, Mohammad S, Baldini G, Mcpike L, Narducci P, Granell S, and Baldini G (2012) Constitutive cholesterol-dependent endocytosis of melanocortin-4 receptor (MC4R) Is essential to maintain receptor responsiveness to α-melanocyte-stimulating Hormone (α-MSH). *J Biol Chem* **287**:21873–21890.

Moore CA, Milano SK, and Benovic JL (2007) Regulation of receptor trafficking by GRKs and arrestins. *Annu Rev Physiol* **69**:451–482.

Nemeth EF (2002) The search for calcium receptor antagonists (calcilytics). *J Mol Endocrinol* **29**:15–21.

Nemeth EF, and Goodman WG (2016) Calcimimetic and calcilytic drugs: feats, flops, and futures.

Nemeth EF, Steffey ME, and Fox J (1996) The parathyroid calcium receptor: A novel therapeutic target for treating hyperparathyroidism. *Pediatr Nephrol* **10**:275–279.

Nørskov-Lauritsen L, Jørgensen S, and Bräuner-Osborne H (2015) N-glycosylation and disulfide bonding affects GPRC6A receptor expression, function, and dimerization. *FEBS Lett* **589**:588–597.

O'Hayre M, Eichel K, Avino S, Zhao X, Steffen DJ, Feng X, Kawakami K, Aoki J, Messer K, Sunahara R, Inoue A, Zastrow M Von, and Gutkind JS (2017) Genetic evidence that β-arrestins are dispensable for the initiation of β2-adrenergic receptor signaling to ERK. *Sci Signal* **10**:eaal3395.

Patel J, and Bridgeman MB (2018) Etelcalcetide (Parsabiv) for secondary hyperparathyroidism in adults with chronic kidney disease on hemodialysis. *P T* **43**:396–399.

Pelkey KA, Yuan X, Lavezzari G, Roche KW, and McBain CJ (2007) mGluR7 undergoes rapid internalization in response to activation by the allosteric agonist AMN082. *Neuropharmacology* **52**:108–117.

Petrel C, Kessler A, Dauban P, Dodd RH, Rognan D, and Ruat M (2004) Positive and negative allosteric modulators of the Ca2+-sensing receptor interact within overlapping but not identical binding sites in the transmembrane domain. *J Biol Chem* **279**:18990–18997.

Pi M, Oakley RH, Gesty-Palmer D, Cruickshank RD, Spurney RF, Luttrell LM, and Quarles LD (2005) β-Arrestin- and G protein receptor kinase-mediated calcium-sensing receptor desensitization. *Mol Endocrinol* **19**:1078–1087.

Reyes-Ibarra AP, García-Regalado A, Ramírez-Rangel I, Esparza-Silva AL, Valadez-Sánchez M, Vázquez-Prado J, and Reyes-Cruz G (2007) Calcium-sensing receptor endocytosis links extracellular calcium signaling to parathyroid hormone-related peptide secretion via a Rab11a-dependent and AMSH-sensitive mechanism. *Mol Endocrinol* **21**:1394–1407.

Roed SN, No AC, Wismann P, Iversen H, Bräuner-Osborne H, Knudsen SM, and Waldhoer M (2015) Functional consequences of glucagon-like peptide-1 receptor cross-talk and trafficking. *J Biol Chem* **290**:1233–1243.

Roed SN, Wismann P, Underwood CR, Kulahin N, Iversen H, Cappelen KA, Schäffer L, Lehtonen J, Hecksher-Soerensen J, Secher A, Mathiesen JM, Bräuner-Osborne H, Whistler JL, Knudsen SM, and Waldhoer M (2014) Real-time trafficking and signaling of the glucagon-like peptide-1 receptor. *Mol Cell Endocrinol* **382**:938–949.

Schrage R, Schmitz AL, Gaffal E, Annala S, Kehraus S, Wenzel D, Büllesbach KM, Bald T, Inoue A, Shinjo Y, Galandrin S, Shridhar N, Hesse M, Grundmann M, Merten N, Charpentier TH, Martz M, Butcher AJ, Slodczyk T, Armando S, Effern M, Namkung Y, Jenkins L, Horn V, Stößel A, Dargatz H, Tietze D, Imhof D, Galés C, Drewke C, Müller CE, Hölzel M, Milligan G, Tobin AB, Gomeza J, Dohlman HG, Sondek J, Harden TK, Bouvier M, Laporte SA, Aoki J, Fleischmann BK, Mohr K, König GM, Tüting T, and Kostenis E (2015) The experimental power of FR900359 to study Gq-regulated biological processes. *Nat Commun* **6**:1–17.

Tennakoon S, Aggarwal A, and Kállay E (2016) The calcium-sensing receptor and the hallmarks of cancer. *Biochim Biophys Acta* **1863**:1398–1407, The Authors.

Thomsen A, Smajilovic S, and Bräuner-Osborne H (2012) Novel strategies in drug discovery of the calcium-sensing receptor based on biased signaling. *Curr Drug Targets* **13**:1324–1335.

Thomsen C, Hansen L, and Suzdak PD (1994) L-Glutamate uptake inhibitors may stimulate phosphoinositide hydrolysis in baby hamster kidney cells expressing mGluR1a via

heteroexchange with L-glutamate without direct activation of mGluR1a. *J Neurochem* **63**:2038–2047.

Trivedi RR, and Bhattacharyya S (2012) Constitutive internalization and recycling of metabotropic glutamate receptor 5 (mGluR5). *Biochem Biophys Res Commun* **427**:185–190.

Vargas KJ, Terunuma M, Tello JA, Pangalos MN, and Moss SJ (2008) The availability of surface GABA B receptors Is independent of gamma-aminobutyric acid but controlled by glutamate in central neurons. *J Biol Chem* **283**:24641–24648.

Ward DT, and Riccardi D (2012) New concepts in calcium-sensing receptor pharmacology and signalling.

White E, McKenna J, Cavanaugh A, and Breitwieser GE (2009) Pharmacochaperone-mediated rescue of calcium-sensing receptor loss-of-function mutants. *Mol Endocrinol* **23**:1115–1123.

Xipell M, Montagud-Marrahi E, Rubio MV, Ojeda R, Arias-Guillén M, Fontseré N, Rodas L, Vera M, Broseta JJ, Torregrosa V, Filella X, and Maduell F (2019) Improved control of secondary hyperparathyroidism in hemodialysis patients switching from oral cinacalcet to intravenous etelcalcetide, especially in nonadherent patients. *Blood Purif* In press.

Yeatman HR, Lane JR, Choy KHC, Lambert NA, Sexton PM, Christopoulos A, and Canals M (2014) Allosteric modulation of M1 muscarinic acetylcholine receptor internalization and subcellular trafficking. *J Biol Chem* **289**:15856–15866.

Zhang C, Zhang T, Zou J, Miller CL, Gorkhali R, Yang JY, Schilmiller A, Wang S, Huang K, Brown EM, Moremen KW, Hu J, and Yang JJ (2016) Structural basis for regulation of human calcium-sensing receptor by magnesium ions and an unexpected tryptophan derivative co-agonist. *Sci Adv* **2**:e1600241.

Zhuang X, Northup JK, and Ray K (2012) Large putative PEST-like sequence motif at the carboxyl tail of human calcium receptor directs lysosomal degradation and regulates cell surface receptor level. *J Biol Chem* **287**:4165–4176.

Footnotes

This project has received funding from the European Union's Horizon 2020 research and innovation programme under grant agreement NO 675228, the Lundbeck Foundation, the Carlsberg Foundation, the Augustinus Foundation and the Toyota Foundation.

Prof. Hans Bräuner-Osborne

Department of Drug Design and Pharmacology

Faculty of Health and Medical Sciences

University of Copenhagen

Universitetsparken 2

DK-2100 Copenhagen, Denmark

E-mail: hbo@sund.ku.dk

[1] These authors contributed equally to this work

Molecular Pharmacology Fast Forward. Published on August 9, 2019 as DOI: 10.1124/mol.119.116772
This article has not been copyedited and formatted. The final version may differ from this version.

Figure legends

Figure 1. Characterization of WT and mutant CaSR constructs. WT and mutant CaSR transiently expressed in HEK293T cells were validated in an IP_1 accumulation assay and by expression analysis. (A) IP_1 accumulation measured after 30 min stimulation with increasing Ca^{2+} concentrations. Data represent mean ± S.E.M. of three independent experiments performed in triplicate. (B) Cell-surface expression of FLAG-SNAP-tagged CaSR WT and mutant constructs obtained with anti-FLAG antibodies in ELISA. Data are mean ± S.E.M. of four experiments performed in parallel with the IP_1 accumulation or internalization assay. The expression of CaSR WT was set to 100% and mutants were compared to CaSR WT using a one-way ANOVA followed by a Dunnett's post-test. (*** $P < 0.001$).

Figure 2. CaSR displays constitutive and concentration-dependent Ca^{2+}-mediated internalization. HEK293T cells were transiently transfected with FLAG-SNAP-CaSR wild-type (WT), orthosteric loss-of-function CaSR mutant (S170A) or FLAG-SNAP-β_2AR. (A) Representative real-time traces showing CaSR WT internalization in response to buffer and increasing Ca^{2+} concentrations. (B) Area under the curve (AUC) plotted against the Ca^{2+} concentration. Data are mean ± S.E.M. of four independent internalization experiments performed in triplicate. (C) Representative real-time traces and (D) baseline-corrected AUC data grouped from three independent experiments of β_2AR internalization upon stimulation with 1 μM isoproterenol in the absence and presence of 0.5 mM or 1 mM EDTA. (E) - (H) The effect of 0.5 mM EDTA on (E) and (F) CaSR WT as well as (G) and (H) CaSR S170A internalization was measured in the absence (open symbols, constitutive internalization) or presence (closed symbols, Ca^{2+}-mediated internalization) of 10 mM Ca^{2+}. (E) and (G) show representative real-time traces and (F) and (H) normalized baseline-corrected AUC data grouped from three independent experiments performed in triplicate. Real-time internalization traces are presented as mean ± S.D. of a single representative experiment performed in triplicate. Statistical analysis was performed using a one-way ANOVA followed by a Dunnett's post-test for (D) and a one-way ANOVA followed by a Tukey's

Molecular Pharmacology Fast Forward. Published on August 9, 2019 as DOI: 10.1124/mol.119.116772
This article has not been copyedited and formatted. The final version may differ from this version.

multiple comparisons test for (F) and (H). Significance is notated as: * $P < 0.05$, ** $P < 0.01$, *** $P < 0.001$.

Figure 3. CaSR internalization is allosterically modulated. Real-time internalization traces of HEK293T cells transiently transfected with FLAG-SNAP-CaSR WT in response to increasing Ca^{2+} concentrations (A) without allosteric modulators, (B) in the presence of 5 μM NPS 2143 and (C) in the presence of 5 μM NPS R-568. (D) Real-time internalization traces for increasing Ca^{2+} concentrations without allosteric modulators recorded from HEK293T cells transiently transfected with FLAG-SNAP-CaSR E837A. Data are mean ± S.D. of a single representative experiment performed in triplicate. (E) Area under the curve (AUC) plotted against the Ca^{2+} concentration. Data are mean ± S.E.M. of three or four independent internalization experiments performed in triplicate.

Figure 4. The CaSR allosteric site E837A mutant abolishes NPS 2143-induced inhibition of Ca^{2+}-mediated CaSR internalization. (A) IP_1 accumulation of CaSR WT upon stimulation with 4 mM Ca^{2+} and increasing NPS 2143 concentrations. (B) IP_1 accumulation for CaSR WT and CaSR E837A upon stimulation with increasing Ca^{2+} concentrations in the absence or presence of 5 μM NPS 2143. (A) and (B), data are mean ± S.E.M. of three independent experiments performed in triplicate. (C) - (F) The effect of NPS 2143 on (C) and (D) CaSR WT as well as (E) and (F) CaSR E837A internalization was measured in the absence (open symbols, constitutive internalization) or presence (closed symbols, Ca^{2+}-mediated internalization) of 10 mM Ca^{2+}. (C) and (E) real-time traces and (D) and (F) normalized baseline-corrected AUC data grouped from three independent experiments performed in triplicate. Statistical analysis was performed using a one-way ANOVA followed by a Tukey's multiple comparisons test. Real-time internalization traces are presented as mean ± S.D. of a single representative experiment performed in triplicate. Significance is notated as: * $P < 0.05$, *** $P < 0.001$.

Figure 5. The CaSR allosteric site E837A mutant abolishes NPS R-568-induced potentiation of constitutive and Ca^{2+}-mediated CaSR internalization. (A) IP_1 accumulation of CaSR WT upon

stimulation with 2 mM Ca^{2+} and increasing NPS R-568 concentrations. (B) IP_1 accumulation for CaSR WT and CaSR E837A upon stimulation with increasing Ca^{2+} concentrations in the absence or presence of 5 μM NPS R-568. Data are mean ± S.E.M. of three independent experiments performed in triplicate. (C) – (F) The effect of NPS R-568 on CaSR WT (C and D) as well as CaSR E837A internalization (E and F) was measured in the absence (open symbols, constitutive internalization) or presence (closed symbols, Ca^{2+}-mediated internalization) of 2 mM Ca^{2+}. (C and E) real-time traces and (D and F) normalized baseline-corrected AUC data grouped from three independent experiments performed in triplicate. Statistical analysis was performed using a one-way ANOVA followed by a Tukey's multiple comparisons test. Real-time internalization traces are presented as mean ± S.D. of a single representative experiment performed in triplicate. Significance is notated as: * $P < 0.05$, *** $P < 0.001$.

Figure 6. CaSR internalization is largely independent on G protein activation. HEK293T cells transiently transfected with FLAG-SNAP-CaSR WT were pre-treated for 30 min with 1 μM $G_{q/11}$ inhibitor YM-254890 or 24h with 80 ng/mL $G_{i/o}$ inhibitor PTX. (A) Normalized IP_1 accumulation upon stimulation with 10 mM Ca^{2+} in the absence or presence of YM-254890. (B) Normalized cAMP accumulation upon stimulation with 10 mM Ca^{2+} in the absence or presence of PTX. (C) Real-time traces in the absence or presence of the G protein inhibitors for constitutive internalization (0 mM Ca^{2+}, open symbols) and Ca^{2+}-mediated internalization (10 mM Ca^{2+}, closed symbols). (D) Normalized grouped AUC data for constitutive and Ca^{2+}-mediated internalization. (E) Constitutive and (F) Ca^{2+}-mediated real-time internalization traces of FLAG-SNAP-CaSR WT transiently transfected in HEK293A or $G_{q/11}$ KO cells. (G) Normalized grouped AUC data after donor signal correction for constitutive and Ca^{2+}-mediated internalization. Data in (A), (B), (D) and (G) are mean ± S.E.M. from three to five independent experiments performed in triplicate. Real-time data in (C), (E) and (F) are mean ± S.D. of a single representative experiment performed in triplicate. Statistical analysis was performed using a one-way ANOVA followed by a Tukey's multiple comparisons test for (A), (B) and (G) and a one-way ANOVA followed by a Dunnett's post-test for (D) (* $P < 0.05$, ** $P < 0.01$, *** $P < 0.001$).

Molecular Pharmacology Fast Forward. Published on August 9, 2019 as DOI: 10.1124/mol.119.116772
This article has not been copyedited and formatted. The final version may differ from this version.

Figure 7. Constitutive and Ca^{2+}-mediated CaSR internalization are β-arrestin1/2-dependent. The β-arrestin1/2 KO cells and HEK239A cells were transiently transfected with FLAG-SNAP-CaSR WT. (A) Constitutive (0 mM Ca^{2+}, open symbols) and Ca^{2+}-mediated (10 mM Ca^{2+}, closed symbols) real-time traces of β-arrestin1/2 KO cells and HEK293A cells. Similar results were generated in at least two additional experiments. (B) Constitutive (0 mM Ca^{2+}, open symbols) and (C) Ca^{2+}-mediated (10 mM Ca^{2+}, closed symbols) real-time internalization traces of β-arrestin1/2 KO cells transiently co-transfected with empty vector, β-arrestin1, β-arrestin2 or a combination of both subtypes (β-arrestin1/2). (D) Normalized grouped AUC data for constitutive and Ca^{2+}-mediated internalization analyzed using a one-way ANOVA followed by a Dunnett's post-test (* $P < 0.05$, ** $P < 0.01$, *** $P < 0.001$). Real-time data presented in (A-C) are mean ± S.D. of a single representative experiment performed in triplicate, while AUC data in (D) are shown as mean ± S.E.M. of three independent experiments performed in triplicate.

Figure 8. CaSR signaling in β-arrestin1/2 KO cells is still sensitive to allosteric modulation. The β-arrestin1/2 KO cells and HEK239A cells were transiently transfected with FLAG-SNAP-CaSR WT. (A) IP_1 accumulation of CaSR WT after 30 min stimulation with increasing Ca^{2+} concentrations in the absence or presence of 5 μM NPS 2143 or NPS R-568. (B) Cell-surface expression of CaSR WT measured using anti-FLAG antibodies in ELISA. Data are mean ± S.E.M. of three experiments performed in parallel with the IP_1 accumulation assay. Statistical analysis was performed using a one-way ANOVA followed by a Tukey's multiple comparisons test. Significance is notated as: *** $P < 0.001$.

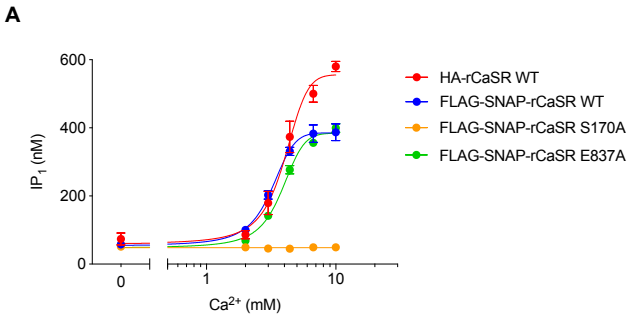
A
600
400
200
0
IP1 (nM)
0
1
10
Ca2+ (mM)
HA-rCaSR WT
FLAG-SNAP-rCaSR WT
FLAG-SNAP-rCaSR S170A
FLAG-SNAP-rCaSR E837A

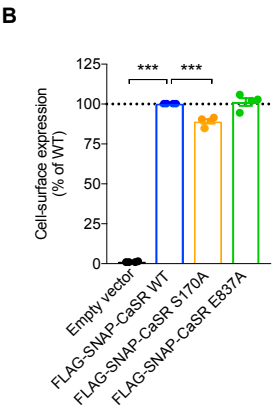
B
125
100
75
50
25
0
Cell-surface expression
(% of WT)
***
***
Empty vector
FLAG-SNAP-CaSR WT
FLAG-SNAP-CaSR S170A
FLAG-SNAP-CaSR E837A

Figure 1

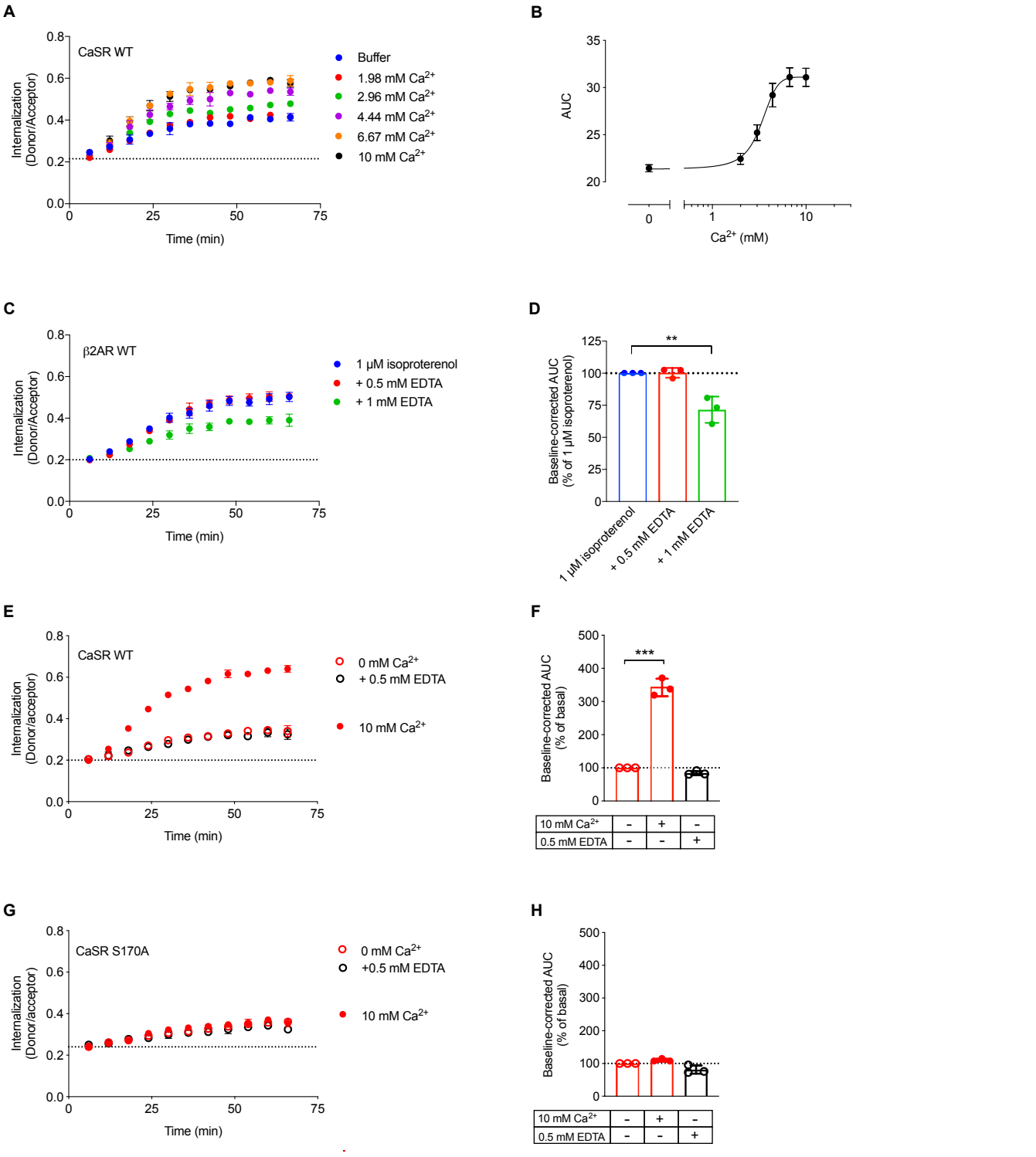
A
CaSR WT
Internalization (Donor/Acceptor)
Time (min)
Buffer
1.98 mM Ca2+
2.96 mM Ca2+
4.44 mM Ca2+
6.67 mM Ca2+
10 mM Ca2+
B
AUC
Ca2+ (mM)
C
β2AR WT
Internalization (Donor/Acceptor)
Time (min)
1 μM isoproterenol
+ 0.5 mM EDTA
+ 1 mM EDTA
D
Baseline-corrected AUC (% of 1 μM isoproterenol)
**
1 μM isoproterenol
+ 0.5 mM EDTA
+ 1 mM EDTA
E
CaSR WT
Internalization (Donor/acceptor)
Time (min)
0 mM Ca2+
+ 0.5 mM EDTA
10 mM Ca2+
F
Baseline-corrected AUC (% of basal)
***
10 mM Ca2+
0.5 mM EDTA
G
CaSR S170A
Internalization (Donor/acceptor)
Time (min)
0 mM Ca2+
+0.5 mM EDTA
10 mM Ca2+
H
Baseline-corrected AUC (% of basal)
10 mM Ca2+
0.5 mM EDTA

Figure 2

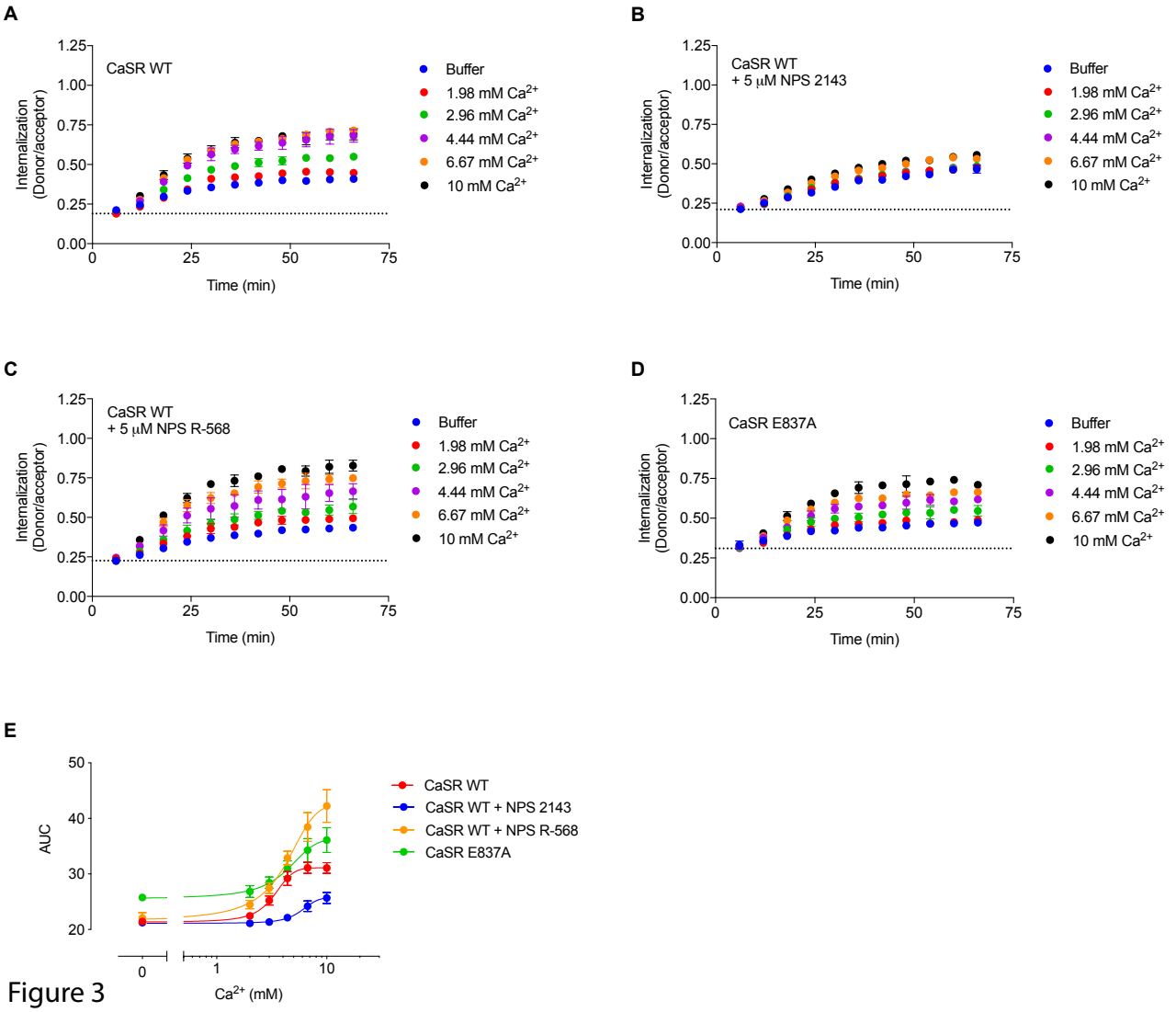
A
CaSR WT
Internalization (Donor/acceptor)
Time (min)
Buffer
1.98 mM Ca2+
2.96 mM Ca2+
4.44 mM Ca2+
6.67 mM Ca2+
10 mM Ca2+
B
CaSR WT
+ 5 μM NPS 2143
C
CaSR WT
+ 5 μM NPS R-568
D
CaSR E837A
E
AUC
Ca2+ (mM)
CaSR WT
CaSR WT + NPS 2143
CaSR WT + NPS R-568
CaSR E837A

Figure 3

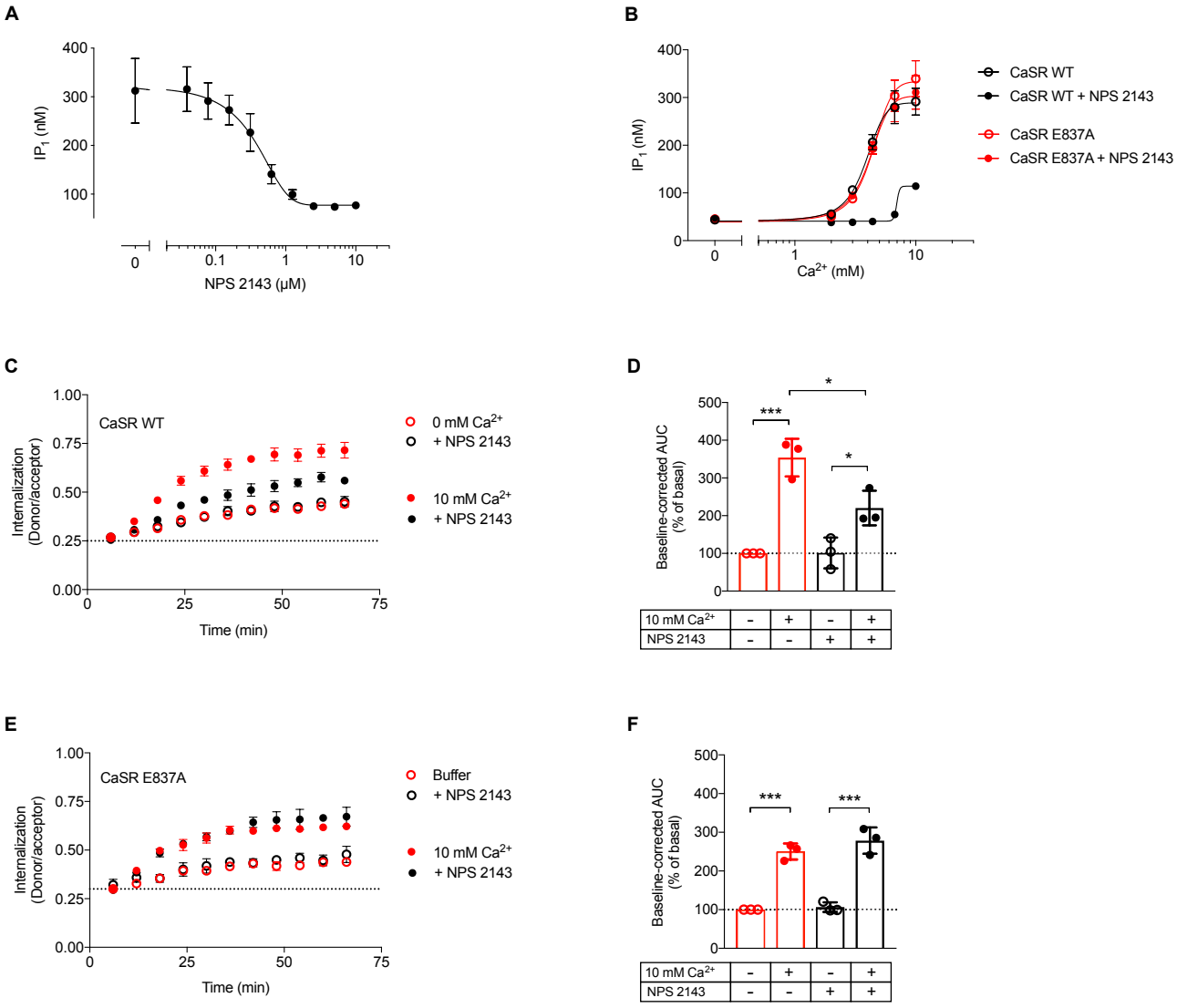
A
IP1 (nM)
NPS 2143 (μM)
B
IP1 (nM)
Ca2+ (mM)
CaSR WT
CaSR WT + NPS 2143
CaSR E837A
CaSR E837A + NPS 2143
C
CaSR WT
Internalization (Donor/acceptor)
Time (min)
0 mM Ca2+
+ NPS 2143
10 mM Ca2+
+ NPS 2143
D
Baseline-corrected AUC (% of basal)
10 mM Ca2+
NPS 2143
E
CaSR E837A
Internalization (Donor/acceptor)
Time (min)
Buffer
+ NPS 2143
10 mM Ca2+
+ NPS 2143
F
Baseline-corrected AUC (% of basal)
10 mM Ca2+
NPS 2143

Figure 4

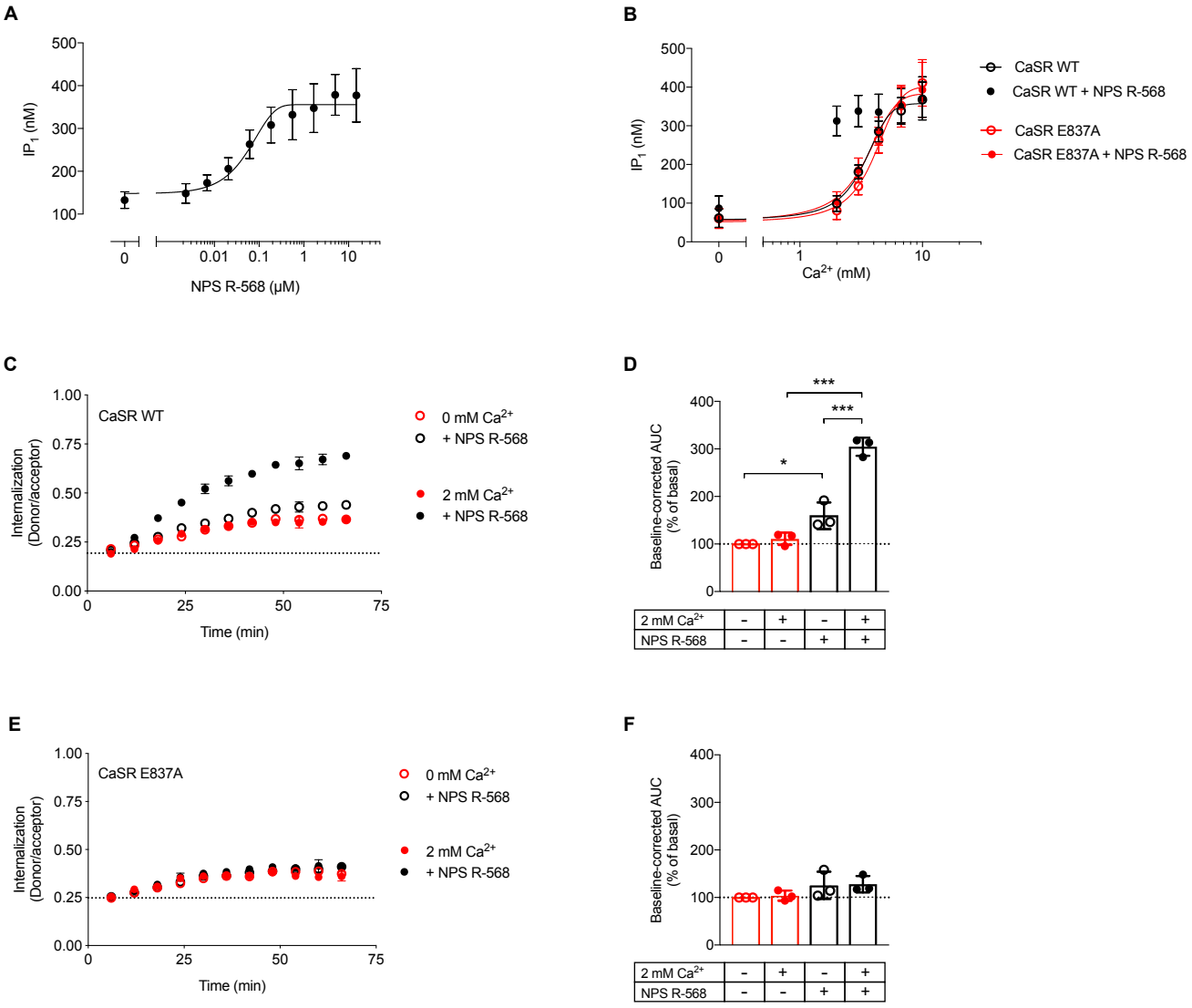
A
IP1 (nM)
NPS R-568 (μM)
B
IP1 (nM)
Ca2+ (mM)
CaSR WT
CaSR WT + NPS R-568
CaSR E837A
CaSR E837A + NPS R-568
C
CaSR WT
Internalization (Donor/acceptor)
Time (min)
0 mM Ca2+
+ NPS R-568
2 mM Ca2+
+ NPS R-568
D
Baseline-corrected AUC (% of basal)
2 mM Ca2+
NPS R-568
E
CaSR E837A
Internalization (Donor/acceptor)
Time (min)
0 mM Ca2+
+ NPS R-568
2 mM Ca2+
+ NPS R-568
F
Baseline-corrected AUC (% of basal)
2 mM Ca2+
NPS R-568

Figure 5

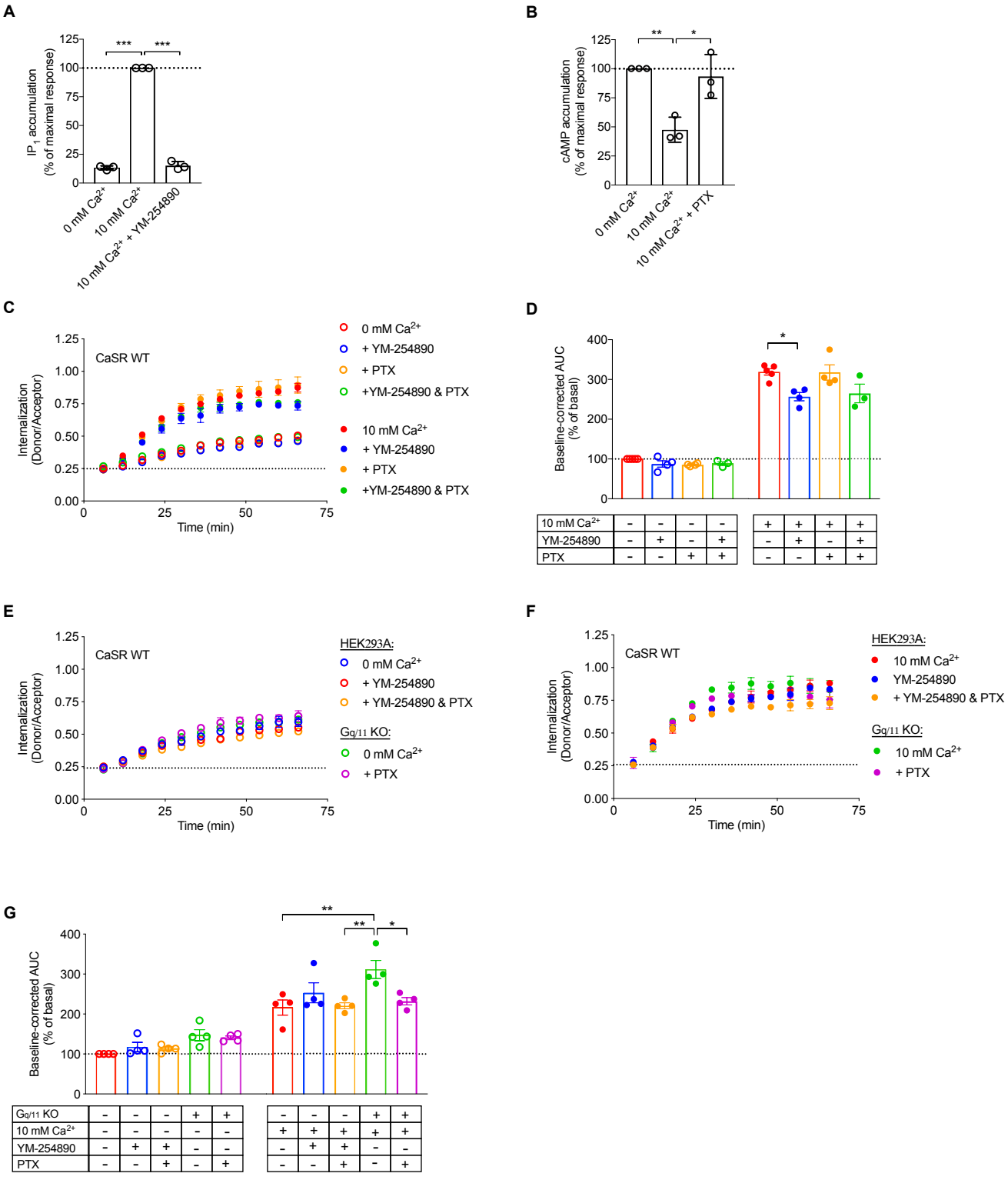
A
IP1 accumulation (% of maximal response)
0 mM Ca2+
10 mM Ca2+
10 mM Ca2+ + YM-254890
B
cAMP accumulation (% of maximal response)
0 mM Ca2+
10 mM Ca2+
10 mM Ca2+ + PTX
C
CaSR WT
Internalization (Donor/Acceptor)
Time (min)
0 mM Ca2+
+ YM-254890
+ PTX
+YM-254890 & PTX
10 mM Ca2+
+ YM-254890
+ PTX
+YM-254890 & PTX
D
Baseline-corrected AUC (% of basal)
10 mM Ca2+
YM-254890
PTX
E
CaSR WT
Internalization (Donor/Acceptor)
Time (min)
HEK293A:
0 mM Ca2+
+ YM-254890
+ YM-254890 & PTX
Gq/11 KO:
0 mM Ca2+
+ PTX
F
CaSR WT
Internalization (Donor/Acceptor)
Time (min)
HEK293A:
10 mM Ca2+
YM-254890
+ YM-254890 & PTX
Gq/11 KO:
10 mM Ca2+
+ PTX
G
Baseline-corrected AUC (% of basal)
Gq/11 KO
10 mM Ca2+
YM-254890
PTX

Figure 6

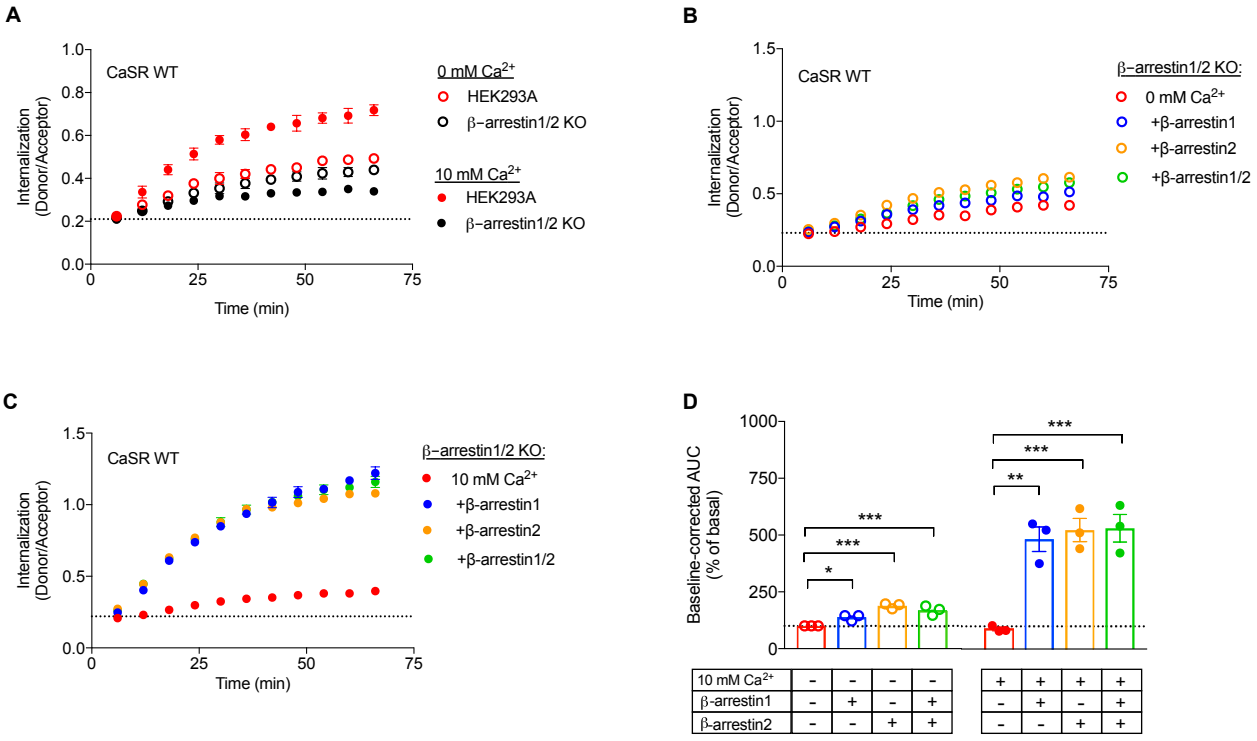
A
CaSR WT
Internalization (Donor/Acceptor)
Time (min)
0 mM Ca2+
HEK293A
β-arrestin1/2 KO
10 mM Ca2+
HEK293A
β-arrestin1/2 KO
B
CaSR WT
Internalization (Donor/Acceptor)
Time (min)
β-arrestin1/2 KO:
0 mM Ca2+
+β-arrestin1
+β-arrestin2
+β-arrestin1/2
C
CaSR WT
Internalization (Donor/Acceptor)
Time (min)
β-arrestin1/2 KO:
10 mM Ca2+
+β-arrestin1
+β-arrestin2
+β-arrestin1/2
D
Baseline-corrected AUC (% of basal)
10 mM Ca2+
β-arrestin1
β-arrestin2

Figure 7

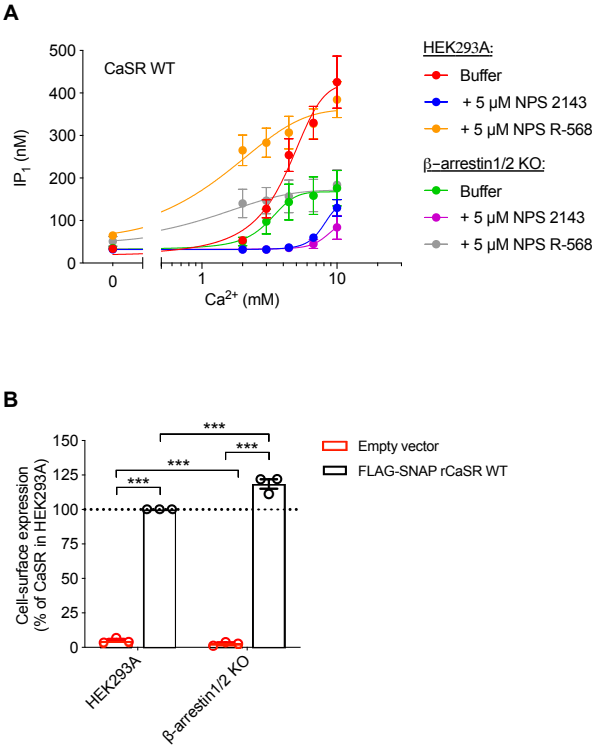
A
CaSR WT
IP1 (nM)
500
400
300
200
100
0
0
1
10
Ca2+ (mM)
HEK293A:
Buffer
+ 5 μM NPS 2143
+ 5 μM NPS R-568
β−arrestin1/2 KO:
Buffer
+ 5 μM NPS 2143
+ 5 μM NPS R-568
B
Cell-surface expression
(% of CaSR in HEK293A)
150
125
100
75
50
25
0
***
***
***
***
Empty vector
FLAG-SNAP rCaSR WT
HEK293A
β-arrestin1/2 KO

Figure 8